PROCEEDINGS B

royalsocietypublishing.org/journal/rspb

Research

Cite this article: Delecambre Z *et al*. 2026 Weak trophic position–body mass relationships undermine simple size-spectrum models for coral reefs. *Proc. R. Soc. B* **293**: 20252357.
https://doi.org/10.1098/rspb.2025.2357

Received: 11 September 2025
Accepted: 19 December 2025

Subject Category:
Ecology

Subject Areas:
ecology, ecosystem

Keywords:
trophic position, biomass pyramid, size spectrum, community, stable isotopes

Author for correspondence:
Zoé Delecambre
e-mail: delecambrezoe@gmail.com

Electronic supplementary material is available online at https://doi.org/10.6084/m9.figshare.c.8257816.

THE ROYAL SOCIETY PUBLISHING

Weak trophic position–body mass relationships undermine simple size-spectrum models for coral reefs

Zoé Delecambre[1], Mattia Ghilardi[1], Diego R. Barneche[2,3], Mehdi Adjeroud[4], Simon J. Brandl[5], Jordan M. Casey[5], Michel Kulbicki[1], Alexandre Mercière[1], Renato A. Morais[1], Fabien Morat[1], Emma Paul Costesec[1,6], Nina M. D. Schiettekatte[7,8], Jason Vii[1], Yves Letourneur[9] and Valeriano Parravicini[1]

[1]Université Paris Sciences et Lettres, CRIOBE, UAR 3278, EPHE-CNRS-UPVD, Avenue Paul Alduy, Perpignan 66100, France
[2]Australian Institute of Marine Science, Indian Ocean Marine Research Centre, Crawley, Western Australia, Australia
[3]Oceans Institute, The University of Western Australia, Crawley, Western Australia, Australia, The University of Western Australia, Crawley, Western Australia, Australia
[4]UMR Entropie (UR-IRD-IFREMER-UNC), Institut de Recherche pour le Développement, Perpignan, France
[5]Department of Marine Science, The University of Texas at Austin, Marine Science Institute, 750 Channel View Drive, Port Aransas, TX 78373, USA
[6]Marine Biology Lab, Université Libre de Bruxelles, Brussels, Belgium
[7]Hawaii Institute of Marine Biology, University of Hawaii, Kaneohe, Hawaii, USA
[8]MARE Centro de Ciências Do Mar E Do Ambiente, Faculdade de Ciências, Universidade de Lisboa, Lisbon 1749-016, Portugal
[9]UMR Entropie (UR-IRD-IFREMER-UNC), Université de la Nouvelle-Calédonie, Nouméa, New Caledonia

ZD, 0009-0000-6473-9048; MG, 0000-0001-9592-7252; DRB, 0000-0002-4568-2362; MA, 0000-0002-6825-8759; SJB, 0000-0002-6649-2496; JMC, 0000-0002-2434-7207; RAM, 0000-0003-4652-6676; FM, 0000-0002-9925-1437; EPC, 0009-0004-1616-4680; NMDS, 0000-0002-1925-3484; YL, 0000-0003-3157-1976; VP, 0000-0002-3408-1625

Unravelling food web dynamics across biological communities is a central goal of ecology. In size-structured ecosystems, the shape of trophic pyramids is often inferred from their size spectra—the distribution of biomass across body-mass classes. Size-spectrum analysis has become a popular tool to study ecosystem functioning in aquatic ecosystems, including coral reefs. However, the key assumption behind size spectra, that body size directly and positively correlates with trophic position, has rarely been evaluated in these systems. Here, we test this assumption by quantifying body mass, population densities and estimating trophic position from stable isotopes for 325 fish species across four Indo-Pacific locations. Consistent with prior studies, we found a positive relationship between biomass and body mass. However, weak and variable relationships between body mass and trophic position led to higher biomass in primary consumers than in predators, as expected in traditional bottom-heavy or diamond-shaped trophic structures. Our findings thus challenge previous reports of coral reef fish biomass prevalence in higher trophic levels (e.g. inverted biomass pyramids), supporting earlier suggestions that simple size-spectrum models do not adequately represent the trophic structure of reef fish communities.

1. Background

Biomass distribution across trophic positions (TPs) is an emergent property of energy transfer in natural ecosystems [1]. It is often depicted as a pyramid in which primary producers comprise the most biomass at the pyramid

base, while apex predators comprise the least biomass at the top (figure 1A). This pattern emerges from the fact that energy and nutrient transfers across adjacent TPs are inefficient, with an estimated 10% of the energy in one TP being transferred to the next, on average [1–3]. This pattern is assumed to exist across all ecosystems and has been observed from terrestrial [4] to aquatic realms [2,5–8].

In many ecosystems, biomass is negatively correlated with individual body size, creating a consistent size spectrum of abundance, biomass and energy [7,9–12]. These size spectra particularly arise in aquatic ecosystems because aquatic organisms are generally gape constrained and only able to feed on smaller-sized prey. Therefore, in aquatic communities, TP is assumed to be dictated largely by body size. This introduces the expectation that trophic and body size pyramids should have a similar shape and explains why—unlike terrestrial ecosystems—body mass is often used as a proxy for TP (figure 1C) [6,8].

Marine communities are energetically open to external subsidies, which may promote fluid shapes of perceived trophic pyramids, with the emergence of different community structures. The classical, bottom-heavy pyramids arise in ecosystems that strongly depend on local primary production or slightly fished systems [6]. Inverted, top-heavy pyramids can emerge in unexploited systems that rely on substantial external subsidies, such as through small-bodied consumers in kelp forests [7] and predator aggregations on coral reefs [13–15]. By contrast, when secondary consumers are more abundant than expected from a typical pyramid shape but top predators are not, pyramids are spatially subsidized [16,17] and have a 'middle-heavy' shape [18]. However, in marine ecosystems, accurately determining the shape and dynamics of trophic structures is challenging because empirically defining the TP of species requires collecting an often prohibitive number of samples for the analysis of gut contents or stable isotopes [15,19]. Therefore, TP is usually expressed assuming a positive relationship with body size or, at best, using species-specific estimates of TP that do not account for spatial and intraspecific variability, especially for coral reef fishes [5,6,12,20].

Coral reef ecosystems are distinct in that they host herbivores (i.e. primary consumers) across an exceptionally broad body-size spectrum, ranging from the smallest marine herbivorous vertebrate (the goby *Koumansetta rainfordi* with approx. 5.6 cm maximum total length or approx. 2 g body mass [21]) to the bumphead parrotfish (approx. 25 000 g average body mass, [22]). By contrast, many predators are relatively small-bodied, with a mean size of approximately 5 cm total length [15,23]. These and other examples suggest that the emergence of inverted biomass pyramids could also reflect food webs that are only partially size-structured, and where body mass does not consistently reflect TP [12,24]. Stable isotope analysis has been used to infer the relationship between body mass and TP, as well as to estimate community-wide predator-to-prey mass ratios, which can influence the shape of the biomass pyramid [6,10,12]. Yet, this approach has seen limited application to coral reef size-spectrum analysis [12,25,26], leaving the relationship between body size and TP in this system largely untested.

Here, we analyse the relationship between body mass and TP in coral reef fish communities to assess the hypothesis that these systems lack size structuring (figure 1D). To test this, we leverage a large dataset of nitrogen stable isotope signatures ($\delta^{15}N$), including 4781 individuals across 325 coral reef fish species from four locations in the Pacific Ocean (New Caledonia and Society, Gambier and Tuamotu archipelagos in French Polynesia; figure 2), combined with underwater visual surveys (UVS) conducted in the same locations. In particular, we investigate four questions: (i) how is fish biomass distributed across body mass classes on coral reefs? (ii) How is fish biomass distributed across TP classes on coral reefs? (iii) Is reef fish body mass positively related to TP? (iv) How are coral reef fish trophic pyramids shaped?

2. Results

Our results are based on a comprehensive dataset where data on fish abundance, body mass and $\delta^{15}N$ signatures were obtained from 70 sampling sites across four locations in the Pacific (New Caledonia, Society, Tuamotu and Gambier archipelagos; figure 2). Values of body mass and abundance were obtained from 348 surveyed transects, while $\delta^{15}N$ signatures were obtained from a variable number of collected individuals from each location (table 1). To integrate stable isotope data with UVS data, we first modelled the relationship between individual $\delta^{15}N$ values, individual body size and species identity for each location using Bayesian modelling. Then, we predicted $\delta^{15}N$ values for each individual recorded in the UVS dataset, which allowed us to capture ontogenetic shifts in $\delta^{15}N$ values. Predicted individual $\delta^{15}N$ values obtained from this analysis were then converted into TP following Hussey *et al.* [27] and Robinson & Baum [12]. In each location, we separated herbivores from carnivores, and we applied the two models described in Robinson & Baum [12], using baselines from the lowest individual $\delta^{15}N$ value in each category and for each location. This method allowed us to retrieve individual values of TP, used in our main analyses. Further analyses aimed at exploring the structure of fish trophic pyramids were conducted using Bayesian hierarchical models, with biomass aggregated at the transect scale by $\log_{10}$ body mass classes or 0.5 binned TP classes, and with sampling sites and years included as random effects (see §5 for further details).

(a) How is fish biomass distributed across body mass classes on coral reefs?

We first examined the structure of reef fish communities by exploring the distribution of fish biomass across the individual body mass gradient. In particular, we explored the relationship between $\log_{10}$ biomass and $\log_{10}$ body mass classes within transects. We found that the probability for a positive relationship was $P(\text{effect} > 0) = 1$ for all our locations (figure 3A and electronic supplementary material, table S1), indicating a generalized tendency for larger fishes to contribute to community biomass more than smaller fishes. All our models had good to moderate explanatory power, with the highest and lowest R^2 in the Tuamotu archipelago and in New Caledonia, respectively ($R^2 = 0.62$ and 0.34; electronic supplementary material, table S1).

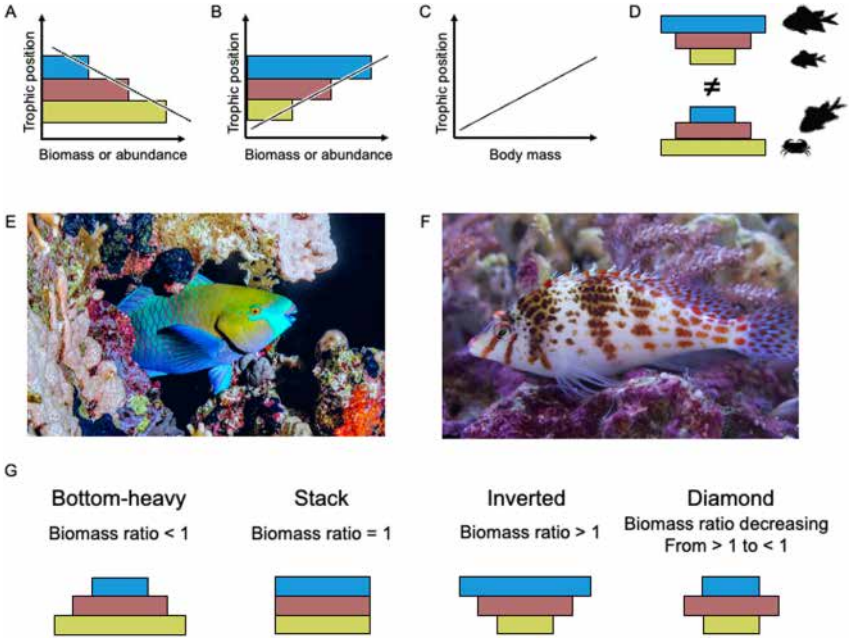

Figure 1. (A) Theoretical relationship between TP and biomass/abundance in a bottom-heavy pyramid. (B) Theoretical relationship between TP and biomass/abundance in an inverted, top-heavy pyramid. (C) Commonly assumed positive relationship between TP and individual body mass. (D) Hypothesized mismatch between body mass-based pyramid (top) and TP-based pyramid (bottom) when the relationship between TP and body mass would not be positive (i.e. body mass would not be a reliable proxy of TP). (E) Example of a large-bodied herbivore, *Scarus quoyi* (average body size = 30 cm), and (F) a small-bodied predator, *Cirrhitichthys falco* (average body size = 6 cm). (G) Theoretical trophic pyramid structures with different biomass ratios between two consecutive TPs. Images: Cinzia Osele Bismarck (E) and James Lee (F).

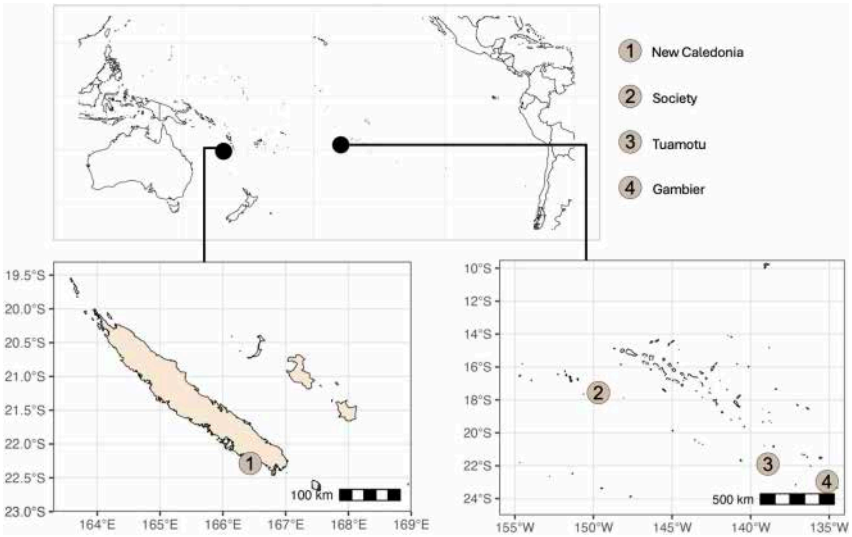

Figure 2. The four study locations: (1) Nouméa, New Caledonia; (2) Mo'orea, Society Islands; (3) Mururoa, Tuamotu Islands; and (4) Mangareva, Gambier Islands.

(b) How is fish biomass distributed across trophic position classes on coral reefs?

We then assessed the shape of the trophic pyramid based on $\log_{10}$ biomass and TP (using TP classes with a bin width of 0.5). Contrary to the expectation, we found a non-positive relationship between $\log_{10}$ biomass and TP classes for three out of four locations (figure 3B and electronic supplementary material, table S1). Only in the Tuamotu did the relationship suggest a positive trend, with $P(\text{effect}_{\text{Tuamotu}} > 0) = 0.92$. However, the explanatory power of these models was considerably lower than those exploring biomass distribution across body mass classes (e.g. between $R^2_{\text{Gambier}} = 0.01$ and $R^2_{\text{Society}} = 0.07$; electronic supplementary material, table S1).

We further explored whether this pattern may have emerged from the method through which we converted δ^{15}N values into TP. More precisely, we assessed the relationship between $\log_{10}$ biomass and raw δ^{15}N classes with a bin width of 1‰ as a sensitivity analysis. The results were largely consistent with those obtained using TP classes, including the trend in the Tuamotu where the probability of a positive relationship between biomass and δ^{15}N classes $P(\text{effect}_{\text{Tuamotu}} > 0)$ was 0.90. However, again, the explanatory power of this set of models was extremely low, with a maximum $R^2 = 0.03$ found in the Tuamotu and Gambier archipelagos (electronic supplementary material, figure S1 and table S2).

Table 1. Summary of the three datasets (UVSs, isotopic signatures and the unification of both) used for the mixed effects models.

database	location	year	number of sites	number of transects	number of species	number of individuals
UVSs	New Caledonia	2010	5	16	169	3379
		2012	6	17	106	1095
	Society	2016	13	78	95	1943
		2018	13	78	98	1830
		2019	13	77	102	2018
	Tuamotu	2006	24	28	148	3296
	Gambier	2010	27	54	170	2900
isotopes	New Caledonia	2010	39		143	1283
	Society	2016	—		48	394
		2018	47		120	518
		2019	31		142	466
	Tuamotu	2006	17		215	2096
	Gambier	2010	29		148	613
assembled dataset	New Caledonia	2010	5	16	54	2908
		2012	6	17	30	711
	Society	2016	13	77	66	1524
		2018	13	78	71	1550
		2019	13	78	69	1314
	Tuamotu	2006	24	28	106	3666
	Gambier	2010	27	54	97	5057

(c) Is coral reef fish body mass positively related to trophic position?

Because community structure differed when assessed by $\log_{10}$ body mass versus TP classes, we further examined the link between individual body mass and TP through Bayesian hierarchical models, treating species as a random effect. We found support for a positive relationship between body mass and TP, with the highest probability of a positive relationship of 0.99 found in New Caledonia and the Society archipelago (figure 3C and electronic supplementary material, table S1). However, the explanatory power of this relationship was extremely low, with the highest value observed in New Caledonia and in the Tuamotu archipelago (R^2 = 0.02), indicating that variation in TP is overwhelmingly not due to variation in body mass. As a result, body mass cannot be considered a reliable proxy for TP. Again, using raw δ^{15}N values instead of TP yielded similar results (electronic supplementary material, figure S1 and table S2).

(d) How are coral reef fish trophic pyramids shaped?

Across locations, the relationship between the biomass ratio of two consecutive TP classes and the midpoint of the upper class was flat to negative (figure 4). Indeed, across all locations, we found evidence against a positive relationship ($P(\text{effect}_{\text{Tuamotu}} > 0)$ = 0.22 to $P(\text{effect}_{\text{Society}} > 0)$ = 0.01; electronic supplementary material, table S1). This is characteristic of pyramids with a higher biomass at the intermediate trophic levels than at the low and high trophic levels (i.e. diamond-shaped trophic structure; figure 1G). Results were consistent using δ^{15}N classes instead of TP classes (electronic supplementary material, figure S1 and table S2).

3. Discussion

By combining UVS and stable isotope analyses, we assessed the extent to which coral reef fish communities are size-structured and whether size spectra can effectively capture ecosystem trophodynamics. We found strong positive relationships between body mass and biomass across four Indo-Pacific locations, consistent with literature reports of inverted biomass pyramids [6,28]. However, we also observed a negative relationship between biomass and TP classes, with TP only weakly associated with body mass. Finally, we showed that the biomass distribution across TP was not linear for reef fishes in our study; rather, biomass pyramids generally exhibited a diamond structure with most biomass accumulated at intermediate trophic levels. Although several models had low explanatory power, which suggests that other factors determine the trophodynamics of fish assemblages, our results clearly show a consistent lack of positive relationship between body size and TP for coral reef fish communities, offering a clearer picture of their trophodynamics in both relatively unexploited (Gambier and Tuamotu archipelagos) and heavily fished reef systems (Society Archipelago and New Caledonia).

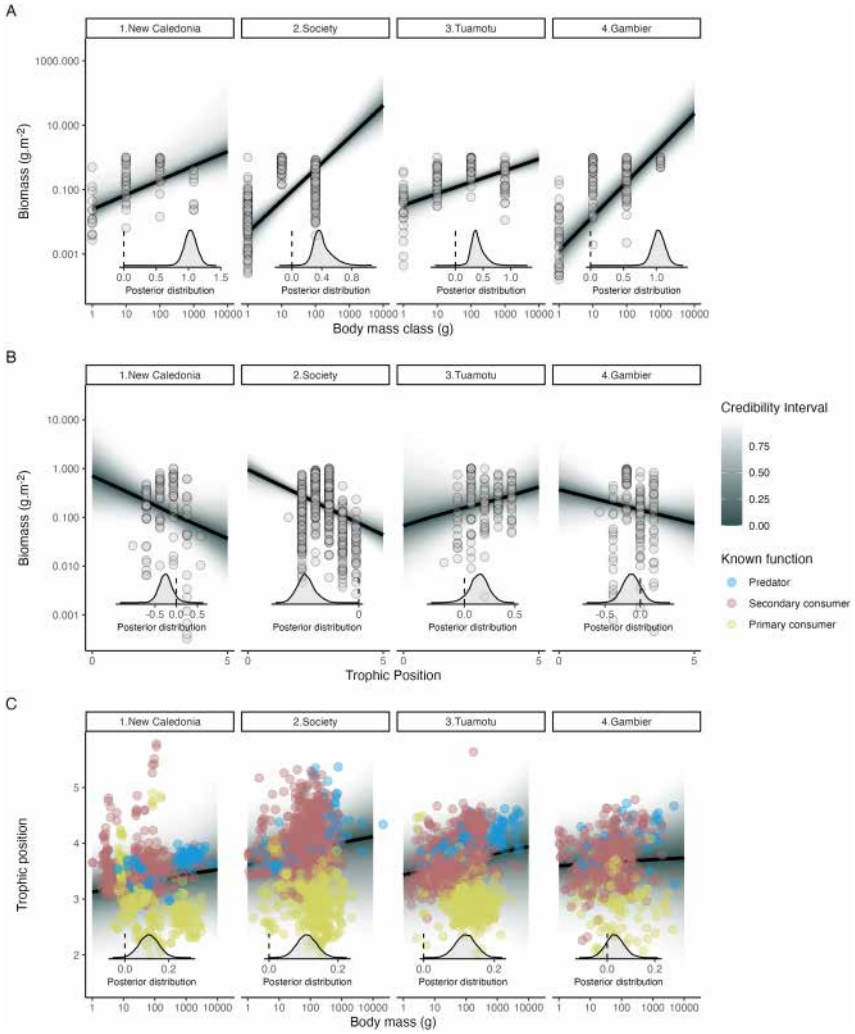

Figure 3. The relationships between biomass and body mass class or TP across the four locations. (A) Transect-level relationships between biomass and body mass classes. (B) Transect-level relationships between biomass and TP classes. For this analysis, the classes of TP (i.e. trophic groups) are defined with a steady step of 0.5. (C) Individual-level relationship between TP and log-transformed body mass. Points represent transects (A and B) or individuals, coloured according to the known trophic guilds (C), while solid lines and ribbons are model predictions and represent the median and credible interval, respectively. Insets illustrate the posterior distribution of the slopes, where the grey area represents the posterior density and vertical, dashed lines represent zero (i.e. no relationship).

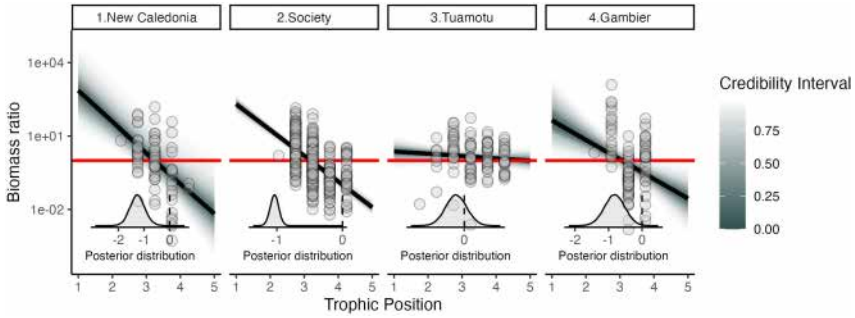

Figure 4. Relationships between the transect-level biomass ratio between two consecutive TP classes and the midpoint of the highest of the two consecutive TP classes across the four locations. Points represent individual transects, while solid lines and ribbons are model predictions and represent the median and credible interval, respectively. Red horizontal lines mark 1 on the *y*-axis, referring to the hypotheses enounced in figure 1G. Insets illustrate the posterior distribution of the slopes, where the grey area represents the posterior density and vertical, dashed lines represent zero (i.e. no relationship).

In unfished conditions, reef fish biomass is sometimes hypothesized to accumulate at higher trophic levels—leading to supposedly 'inverted' (or top-heavy) biomass pyramids [6]. In line with this hypothesis, our results illustrate how such inverted biomass pyramids might emerge [29,30]. This pattern has traditionally been associated with predator-dominated, isolated and uninhabited ecosystems, which are often contrasted with overfished and 'trophic downgraded' systems [6,20,31,32]. While inverted pyramid structures are possible and occur in simplified or restricted components of food webs (such as planktonic or insect–bromeliad food webs [20]), they remain unlikely in natural, complex ecosystems such as coral reefs, given the requirements of specific combinations of predator and prey body size ratios, ontogenetic stage of prey and energy transfer efficiency [3,33].

When using TP rather than body mass, we observed the opposite trend, a negative relationship between reef fish biomass and TP classes, despite low explanatory power in the models. On coral reefs, inverted biomass pyramids are typically reported based on observed large proportions of top predators in comparison to organisms at lower TP [31,32]. This observation can be explained by sampling bias [34,35] or failing to account for cross-ecosystem food web connections (i.e. spatial subsidies) [13,29,36]. Top predators on coral reefs (e.g. reef sharks, jacks and trevallies) move across non-reef ecosystems (e.g. pelagic waters, mangroves and seagrass beds) and thus feed across multiple trophic pyramids and levels [36,37]. This 'active subsidizing' behaviour explains how some predators seemingly escape the constraints of decreasing biomass transfer efficiency, but it may also inflate the perceived top-level biomass within any single food web [6,35,38]. Our study only focuses on ray-finned fish species to remove the biases associated with sharks, which might not be gape-limited. Both mobile predators, such as trevallies and snappers, and subsidies from prey movements (e.g. planktonic inputs [16]) can also skew local biomass pyramids [19,28]. The most parsimonious interpretation of our findings is that body mass and TP are decoupled in reef fishes. This is driven, at least in part, by low TP-feeding fishes that have large body sizes [33].

On coral reefs, species that occur at low TP can often outgrow species that occur at high TP. For instance, parrotfishes are low-TP consumers that predominantly feed on algae and cyanobacteria [14,32] (figure 1E); yet, the steephead parrotfish, *Chlorurus microrhinos*, can reach 70 cm in length and 5 kg in weight [39–41]. On the other hand, several families of piscivorous predators rarely exceed 30 cm (e.g. Synodontidae [42], Cirrhitidae [43]; figure 1F), and most cryptobenthic predators grow no more than a few centimetres in length [23]. Such mismatches between TP and body mass may help explain why some coral reef food webs appear to exhibit inverted trophic pyramids when solely based on body mass [20,33]. Predation on coral reefs is largely driven by small-bodied predators, including cryptopredators under 15 cm in length, which account for up to 90% of predation events [23]. Their dominance is supported by the high productivity and turnover of cryptobenthic fishes, which provide a constant, abundant prey base despite their small size [44]. These dynamics allow small predators to play a major trophic role, decoupling body size from predation pressure. In contrast, the prevalence of large-bodied herbivores likely reflects the extensive, fast evolutionary diversification of nominally herbivorous fishes (mostly parrotfishes and surgeonfishes), as well as the potential role of detritus in facilitating their growth [45].

We revealed a negative relationship between biomass ratios and TP classes in almost all studied locations. This pattern illustrates biomass pyramids where the biomass of the primary consumers is equal to or superior to the biomass in the previous layers of the pyramid, whereas the biomass of the secondary consumers at the top of the pyramid is inferior to the biomass of the primary consumers (i.e. diamond-shaped trophic structure; figure 1G). Although literature that supports diamond-shaped trophic pyramid structure is scarce, this type of pyramid highlights generalist predators that feed across TP [33,46], engaging in dietary flexibility, omnivory, intra-guild predation [47] and cannibalism [48]. Finally, diamond-shaped pyramids can, to some extent, also be the consequence of intense human harvesting of large herbivorous and predatory fishes. Regardless of the mechanism, this showcases that traditional trophic pyramids may be too simple to characterize the full complexity of coral reef fish communities. Although our study considered only fish consumers, excluding producers and invertebrate consumers, accounting for these lower trophic levels would likely further support the view that inverted biomass pyramids are uncommon on coral reefs [26,49].

Our findings are also relevant to coral reef energetics. For example, the fact that many predators are small-bodied and consume small prey [23], including detritivorous cryptobenthic fishes, points to the prominence of nutrient cycling in shaping the food chain [50]. Moreover, the diamond-shaped structure of some systems suggests a strong reliance on invertebrates, sourced from the benthos or pelagic zone, supporting evidence that reef trophic structure is frequently subsidized by pelagic sources [6,17,51,52]. Finally, bottom-heavy pyramids support a more classic interpretation of Lindeman's pyramid [1], indicating that some systems might be fuelled by benthic primary productivity. Therefore, our results reveal a wide diversity of energy acquisition and transfer across reef ecosystems.

Our study has several limitations. First, due to the lack of site-specific isotopic baselines (e.g. algae or pelagic organic matter), TP was estimated relative to the lowest $\delta^{15}N$ values among herbivores and carnivores in each community. Although additional baselines might have improved our TP estimates [19], our approach was necessary given the heterogeneous, large dataset, which lacked consistent baseline data. Another limitation is the explanatory power of some of our models. Exploring the relationships between biomass and TP, TP and body mass, or TP and biomass ratios, for example, generated R^2 values that were lower than the values obtained with body mass classes. The low R^2 may be due to the existence of different and variable energetic pathways that fuel coral reef ecosystems. This complexity makes reefs remarkably different from more closed or simpler ecosystems, whereby the size spectra capture the trophic structure of the ecosystem. Finally, our exclusion of non-fish taxa, especially primary producers and invertebrate consumers, likely leads to an underestimate of the slopes of size spectra [53], although the expected effect of such is dampening of the strong detected body mass–biomass relationships.

4. Conclusion

Our study reveals that coral reef fish food webs are diamond-shaped when TP is empirically estimated through stable isotopes. We suspect that some earlier observations of inverted biomass pyramids may have emerged as artefacts from treating body mass as a surrogate for TP. We hypothesize that the presence of large herbivores and small top predators drives this mismatch between body mass and TP. Our results support recent calls to re-evaluate the assumption that unharvested coral reefs are dominated by top predators and non-top-heavy biomass pyramids emerge predominantly in response to anthropogenic impacts. Therefore, caution must be exercised when evaluating size structures across coral reef food chains. When assumptions are made based on body mass, size structure may lead to biased interpretations of ecosystem functioning.

5. Methods

(a) Data collection

(i) Fish surveys

We compiled fish community data from UVSs conducted across four tropical archipelagos, including New Caledonia and the Society, Gambier and Tuamotu Islands in French Polynesia (figure 2). In the Society Islands, data were collected across eight marine protected areas (MPAs) in Moorea, where UVSs have been conducted annually since 2004 by the Centre de Recherche Insulaire et Observatoire de l'Environnement (CRIOBE) under the Service National d'Observation CORAIL programme (SNO CORAIL). We selected UVS data from 2016, 2018 and 2019 to match the years when stable isotope analyses were conducted. In each MPA, three UVS replicates are performed at each of three reef zones: fringing reef, barrier reef and outer slope. For consistency across archipelagos, we only selected lagoon areas from this survey (i.e. fringing and inner barrier reef). A UVS consists of a 25 × 2 m belt transect where divers record the species, size and abundance of all fishes. In the Gambier and Tuamotu archipelagos of French Polynesia, data collection followed a different but consistent method, with all UVSs in the lagoon. UVSs consisted of 50 × 10 m belt transects along which two divers recorded the species, size and abundance of all fishes. In the Gambier Archipelago, data were collected in 2010 across 20 lagoon sites across all the islands, while in the Tuamotu Islands, four lagoon sites were surveyed around Mururoa Island in 2006. In New Caledonia, 37 sites were surveyed between 2006 and 2019. From these, we selected data from 2010 and 2012 to match the years when stable isotope analyses were conducted. This selection included six sites and 17 transects. Among the four archipelagos sampled, the Gambier Archipelago and Mururoa Island were the least harvested sites, while the Society Archipelago and New Caledonia included the most human-impacted sites (e.g. Moorea and Noumea). We calculated standing biomass across locations by summing biomass across all transects and dividing it by the total area surveyed, thus accounting for differences in belt transect dimensions. Fish lengths were converted to body mass using length–weight coefficients from FishBase [54]. Large predators tend to be overestimated in non-instantaneous counts due to their fast-swimming speeds [35], while small, cryptic fishes are often overlooked by observers [44,55]. Thus, we removed sharks and rays, as well as fish species with body mass estimates of less than 1 g, from the datasets.

(ii) Fish collections and stable isotope analyses

In each archipelago, in the same years when UVSs were conducted, a subset of the surveyed fish species was collected for stable isotope analysis. Collection details for each sampling period are detailed in table 1.

In Moorea, large fishes were collected using spearguns, and small cryptobenthic fishes were collected with a 4 : 1 ethanol to clove oil solution. Across the other archipelagos, fishes were collected with anaesthetic [56]. After collections, dorsal white muscle was sampled to assess the isotopic signature of each individual. Samples were stored in 2 ml tubes at −20°C. Sample vials were covered with parafilm and then freeze-dried for a minimum duration of 24 h. Dried samples were then ground with metal balls in a Tissue Lyser (Qiagen). For samples from the Society Archipelago, encapsulation and mass spectrometry to assess $\delta^{15}N$ was performed at Cornell Stable Isotope Laboratory (COIL). For samples from the Gambier and Tuamotu Islands, analyses were performed at the University of Santa Monica. For the samples from New Caledonia, analyses were performed at the University of Newcastle and the Scottish Crop Research Institute [57].

(b) Data preparation

For each individual fish recorded in the UVS data, we predicted a location and individual-specific $\delta^{15}N$ based on body size to account for ontogenetic shifts in $\delta^{15}N$ values. In each location, for species with more than six $\delta^{15}N$ observations (n = 121 species out of 260 species), $\delta^{15}N$ was predicted using species-specific $\delta^{15}N$–length relationships obtained by fitting a Bayesian linear regression with the *brms* R package [58], with $\delta^{15}N$ as the response variable and a species and $\log_2$ total length interaction as the predictor. For the remaining species (n = 139 species out of 260 species), $\delta^{15}N$ was predicted using $\delta^{15}N$–length relationships modelled at the level of trophic guilds.

We relied on TP values rather than raw $\delta^{15}N$ for our statistical analyses, as estimated in Hussey *et al.* [27] and more recently in Robinson & Baum [12]. Indeed, the fractionation of $\delta^{15}N$ across trophic levels is nonlinear [59], and tools have been developed to approximate reliable estimates of TP values from $\delta^{15}N$. We therefore followed the method found in Robinson & Baum [12] that estimates the TPs of carnivores and herbivores separately as the fractionation can strongly vary between these guilds [12,19,27,59]. This method uses two different modelling approaches, baselines and fractionation values for carnivores and herbivores (as also recommended in [19]): the TP calculation for carnivores relies on a *scaled* method (i.e. allows the fractionation value to depend on the $\delta^{15}N$ limit reached as TP increases) developed in [27]. The value of the $\delta^{15}N$ limit was retrieved from [27] ($\delta^{15}N_{lim}$ = 0.27). On the other hand, the TP estimation for herbivores was calculated through an *additive* method, where fractionation is a set value, calculated in [12] ($\text{fractionation}_{\text{herbivores}}$ = 4.778‰). Following these methods, we used the predicted individual $\delta^{15}N$ values computed from the UVS dataset to run the models. For both herbivores and carnivores, at least one baseline was required to estimate TP values for the rest of the community. Hence, following Robinson & Baum [12], as baselines, we used the $\delta^{15}N$ value of the individual that has the lowest $\delta^{15}N$ value of its community for each guild (herbivore versus carnivore) and location. For example, to estimate the TP values of carnivores with the *scaled* method, we used the $\delta^{15}N$ value of the planktivore with the lowest $\delta^{15}N$ value in the fish community as the single baseline in the model. Similarly, to estimate the TP values of herbivores with the *additive* approach, we used the $\delta^{15}N$ value of the herbivore with the lowest $\delta^{15}N$ value across

the herbivore community as the single baseline. Estimations of TP and the selection of baselines were performed separately for each location. To ensure our results were not strictly dependent on the method used to estimate TP, we kept $\delta^{15}N$ values for sensitivity analyses.

(c) Statistical analyses

Statistical analyses were performed based on the following questions: (i) how is fish biomass distributed across body mass classes on coral reefs? (ii) How is fish biomass distributed across TP classes on coral reefs? (iii) Is coral reef fish body mass positively related to TP? (iv) How are coral reef fish biomass pyramids shaped?

(i) How is fish biomass distributed across body mass classes on coral reefs?

To investigate the relationship between biomass and body mass, we first binned fish biomass for each transect according to logarithmic ($\log_{10}$) body mass classes as described by [10]. We obtained a single value of log-transformed biomass for each body mass class and each transect. Then, for each archipelago, we fitted a Bayesian linear mixed effects model with log-transformed biomass (i.e. the proportion of total transect biomass present in each size class) as the response variable and body mass classes as the explanatory variable. The site was included as a random effect on both the intercept and slope, and year was included as a random effect on the intercept when sampling was performed over multiple years (i.e. in the Society Islands and New Caledonia).

(ii) How is fish biomass distributed across trophic position classes on coral reefs?

To investigate the relationship between biomass and TP, we first binned fish biomass into TP classes and $\delta^{15}N$ classes for sensitivity analysis. Currently, no consensus exists on the best constant width for $\delta^{15}N$ classes [27,59]. Thus, we used a bin width of 1‰ for $\delta^{15}N$ and 0.5 for TP. Then, for each archipelago, we fitted a Bayesian mixed effects model with biomass as the response variable and TP classes as the explanatory variable. As in the previous set of models, site and year were included as random effects. We fitted separate models for each location to account for potential differences in TP and baselines.

(iii) Is coral reef fish body mass positively related to trophic position?

To assess the assumed positive relationship between body mass and TP, we fitted a Bayesian mixed effects model with the individual $\log_{10}$ body mass as the explanatory variable and the individual TP as the response variable from the fish isotope dataset. Here, species was included as a random effect on the intercept and slope. To assess the sensitivity of results to the method used to estimate TP, we repeated the analysis using $\delta^{15}N$ as a response variable.

(iv) How are coral reef fish trophic pyramids shaped?

To identify the shape of the biomass pyramids, we computed the biomass ratio between two consecutive classes of TP (or $\delta^{15}N$ for sensitivity analysis) and used the log-transformed biomass ratio ($\log_{10}$) as the response variable in separate Bayesian mixed effects models for each location. We used the midpoint of the upper TP class as the explanatory variable and included site as a random effect on the intercept and slope, and year as a random effect on the intercept.

(v) Model fitting and evaluation

All analyses were performed using the package *brms* [58] in R [60]. All model sets were implemented by running four independent Markov chain Monte Carlo (MCMC) with 6000 steps per chain, retaining the last 3000 draws of each chain. Default, weakly informative priors were employed for all model parameters with a student distribution on the intercept and a flat distribution on the slopes. For each model, we examined all posterior predictive distributions and trace plots to assess convergence, and R-hat statistics were inspected for each parameter of each model. If the four MCMC have converged, then the R-hat value should not exceed 1. All indicators were deemed satisfactory and are presented in the electronic supplementary material, tables S1 and S2. To evaluate the effects in our models, we used the posterior probability of a positive effect (i.e. proportion of the posterior distribution above zero) of the explanatory variable on the response variable, which would be expected for an inverted trophic pyramid. Effects with a posterior probability over 0.975 or under 0.025 (i.e. equivalent to a 0.95 probability of a negative effect) were deemed significant. In addition to posterior probabilities, the relevance of an effect was estimated by looking at the model R^2 [61], calculated with the *bayes_R2* function in the *rstantools* package [62]. For each model, the R^2 calculation was conditioned on the fixed effects only. An R^2 close to 1 would indicate a high explanatory power of the model, while a R^2 close to 0 indicates a weak explanatory power.

Ethics. This work did not require ethical approval from a human subject or animal welfare committee.

Data accessibility. Raw and processed data are publicly available at [63]. Any additional information required to reanalyse the data reported in this paper is available from the lead contact upon request.

Supplementary material is available online [64].

Declaration of AI use. We have not used AI-assisted technologies in creating this article.

Authors' contributions. Z.D.: conceptualization, formal analysis, investigation, methodology, visualization, writing—original draft, writing—review and editing; M.G.: methodology, visualization, writing—review and editing; D.R.B.: formal analysis, methodology, writing—review and editing; M.A.: writing—review and editing; S.J.B.: writing—review and editing; J.M.C.: supervision, writing—review and editing; M.K.: writing—review and editing; A.M.: writing—review and editing; R.M.: methodology, writing—review and editing; F.M.: writing—review and editing; E.P.C.: writing—review and editing; N.M.D.S.: writing—review and editing; J.V.: conceptualization, methodology, writing—review and editing; Y.L.: conceptualization, methodology, writing—review and editing; V.P.: conceptualization, methodology, resources, supervision, validation, writing—original draft, writing—review and editing.

All authors gave final approval for publication and agreed to be held accountable for the work performed therein.

Conflict of interest declaration. We declare we have no competing interests.

Funding. No funding has been received for this article.

References

1. Lindeman RL. 1942 The trophic-dynamic aspect of ecology. *Ecology* **23**, 399–417. (doi:10.2307/1930126)
2. Eddy TD *et al*. 2021 Energy flow through marine ecosystems: confronting transfer efficiency. *Trends Ecol. Evol.* **36**, 76–86. (doi:10.1016/j.tree.2020.09.006)
3. Barneche DR, Allen AP. 2018 The energetics of fish growth and how it constrains food-web trophic structure. *Ecol. Lett.* **21**, 836–844. (doi:10.1111/ele.12947)
4. Harfoot MBJ, Newbold T, Tittensor DP, Emmott S, Hutton J, Lyutsarev V, Smith MJ, Scharlemann JPW, Purves DW. 2014 Emergent global patterns of ecosystem structure and function from a mechanistic general ecosystem model. *PLoS Biol.* **12**, e1001841. (doi:10.1371/journal.pbio.1001841)
5. Yvon-durocher G, Montoya JM, Trimmer M, Woodward G. 2011 Warming alters the size spectrum and shifts the distribution of biomass in freshwater ecosystems. *Glob. Chang. Biol.* **17**, 1681–1694. (doi:10.1111/j.1365-2486.2010.02321.x)
6. Trebilco R, Baum JK, Salomon AK, Dulvy NK. 2013 Ecosystem ecology: size-based constraints on the pyramids of life. *Trends Ecol. Evol.* **28**, 423–431. (doi:10.1016/j.tree.2013.03.008)
7. Trebilco R, Dulvy NK, Anderson SC, Salomon AK. 2016 The paradox of inverted biomass pyramids in kelp forest fish communities. *Proc. R. Soc. B* **283**, 20160816. (doi:10.1098/rspb.2016.0816)
8. Nagelkerke LAJ, Rossberg AG. 2014 Trophic niche-space imaging, using resource and consumer traits. *Theor. Ecol.* **7**, 423–434. (doi:10.1007/s12080-014-0229-5)
9. Jennings S, Mackinson S. 2003 Abundance–body mass relationships in size-structured food webs. *Ecol. Lett.* **6**, 971–974. (doi:10.1046/j.1461-0248.2003.00529.x)
10. Blanchard JL, Heneghan RF, Everett JD, Trebilco R, Richardson AJ. 2017 From bacteria to whales: using functional size spectra to model marine ecosystems. *Trends Ecol. Evol.* **32**, 174–186. (doi:10.1016/j.tree.2016.12.003)
11. Blanchard J. 2008 The dynamics of size-structured ecosystems. *University of Tasmania* (doi:10.25959/23226071)
12. Robinson JPW, Baum JK. 2016 Trophic roles determine coral reef fish community size structure. *Can. J. Fish. Aquat. Sci.* **73**, 496–505. (doi:10.1139/cjfas-2015-0178)
13. Siqueira AC, Morais RA, Bellwood DR, Cowman PF. 2021 Planktivores as trophic drivers of global coral reef fish diversity patterns. Proc. Natl Acad. Sci. USA **118**, 1–8. (doi:10.1073/pnas.2019404118/-/DCSupplemental)
14. Fey P *et al*. 2021 Multi-trophic markers illuminate the understanding of the functioning of a remote, low coral cover Marquesan coral reef food web. *Sci. Rep.* **11**, 20950. (doi:10.1038/s41598-021-00348-w)
15. Briand MJ, Bonnet X, Guillou G, Letourneur Y. 2016 Complex food webs in highly diversified coral reefs: insights from δ13C and δ15N stable isotopes. *Food Webs* **8**, 12–22. (doi:10.1016/j.fooweb.2016.07.002)
16. Polis GA, Anderson WB, Holt RD. 1997 Toward an integration of landscape and food web ecology: the dynamics of spatially subsidized food webs. *Annu. Rev. Ecol. Syst.* **28**, 289–316. (doi:10.1146/annurev.ecolsys.28.1.289)
17. Morais RA, Siqueira AC, Smallhorn-West PF, Bellwood DR. 2021 Spatial subsidies drive sweet spots of tropical marine biomass production. *PLoS Biol.* **19**, e3001435. (doi:10.1371/journal.pbio.3001435)
18. Skinner C, Mill AC, Fox MD, Newman SP, Zhu Y, Kuhl A, Polunin NVC. 2021 Offshore pelagic subsidies dominate carbon inputs to coral reef predators. *Sci. Adv.* **7**, 1–12. (doi:10.1126/sciadv.abf3792)
19. Letourneur Y, Fey P, Dierking J, Galzin R, Parravicini V. 2024 Challenging trophic position assessments in complex ecosystems: calculation method, choice of baseline, trophic enrichment factors, season and feeding guild do matter: a case study from Marquesas Islands coral reefs. *Ecol. Evol.* **14**, e11620. (doi:10.1002/ece3.11620)
20. McCauley DJ, Gellner G, Martinez ND, Williams RJ, Sandin SA, Micheli F, Mumby PJ, McCann KS. 2018 On the prevalence and dynamics of inverted trophic pyramids and otherwise top-heavy communities. *Ecol. Lett.* **21**, 439–454. (doi:10.1111/ele.12900)
21. Depczynski M, Bellwood D. 2003 The role of cryptobenthic reef fishes in coral reef trophodynamics. *Mar. Ecol. Prog. Ser.* **256**, 183–191. (doi:10.3354/meps256183)
22. Taylor BM, Hamilton RJ, Almany GR, Howard Choat J. 2018 The world's largest parrotfish has slow growth and a complex reproductive ecology. *Coral Reefs* **37**, 1197–1208. (doi:10.1007/s00338-018-1723-9)
23. Mihalitsis M, Morais RA, Bellwood DR. 2022 Small predators dominate fish predation in coral reef communities. *PLoS Biol.* **20**, e3001898. (doi:10.1371/journal.pbio.3001898)
24. Barneche DR, Kulbicki M, Floeter SR, Friedlander AM, Allen AP. 2016 Energetic and ecological constraints on population density of reef fishes. *Proc. R. Soc. B* **283**, 1–8. (doi:10.1098/rspb.2015.2186)
25. Cocheret de la Morinière E, Pollux BJA, Nagelkerken I, Hemminga MA, Huiskes AHL, van der Velde G. 2003 Ontogenetic dietary changes of coral reef fishes in the mangrove–seagrass–reef continuum: stable isotopes and gut-content analysis. *Mar. Ecol. Prog. Ser.* **246**, 279–289. (doi:10.3354/meps246279)
26. Brandl SJ, Yan HF, Casey JM, Schiettekatte NMD, Renzi JJ, Mercière A, Morat F, Côté IM, Parravicini V. 2025 A seascape dichotomy in the role of small consumers for coral reef energy fluxes. *Ecology* **106**, 1–17. (doi:10.1002/ecy.70065)
27. Hussey NE, Macneil MA, McMeans BC, Olin JA, Dudley SFJ, Cliff G, Wintner SP, Fennessy ST, Fisk AT. 2014 Rescaling the trophic structure of marine food webs. *Ecol. Lett.* **17**, 239–250. (doi:10.1111/ele.12226)
28. Barnes C, Maxwell D, Reuman DC, Jennings S. 2010 Global patterns in predator–prey size relationships reveal size dependency of trophic transfer efficiency. *Ecology* **91**, 222–232. (doi:10.1890/08-2061.1)
29. Mourier J, Maynard J, Parravicini V, Ballesta L, Clua E, Domeier ML, Planes S. 2016 Extreme inverted trophic pyramid of reef sharks supported by spawning groupers. *Curr. Biol.* **26**, 2011–2016. (doi:10.1016/j.cub.2016.05.058)

30. Friedlander AM, DeMartini EE. 2002 Contrasts in density, size, and biomass of reef fishes between the northwestern and the main Hawaiian islands: the effects of fishing down apex predators. *Mar. Ecol. Prog. Ser.* **230**, 253–264. (doi:10.3354/meps230253)
31. Friedlander AM, Sandin SA, DeMartini EE, Sala E. 2010 Spatial patterns of the structure of reef fish assemblages at a pristine atoll in the central Pacific. *Mar. Ecol. Prog. Ser.* **410**, 219–231. (doi:10.3354/meps08634)
32. Sandin SA *et al*. 2008 Baselines and degradation of coral reefs in the Northern Line Islands. *PLoS One* **3**, e1548. (doi:10.1371/journal.pone.0001548)
33. Woodson CB, Schramski JR, Joye SB. 2018 A unifying theory for top-heavy ecosystem structure in the ocean. *Nat. Commun.* **9**, 23. (doi:10.1038/s41467-017-02450-y)
34. Fath BD, Killian MC. 2007 The relevance of ecological pyramids in community assemblages. *Ecol. Modell.* **208**, 286–294. (doi:10.1016/j.ecolmodel.2007.06.001)
35. Ward-Paige C, Mills Flemming J, Lotze HK. 2010 Overestimating fish counts by non-instantaneous visual censuses: consequences for population and community descriptions. *PLoS One* **5**, e11722. (doi:10.1371/journal.pone.0011722)
36. McCauley D. 2012 Nature—half lost or half saved? *Science* **337**, 1455–1456. (doi:10.1126/science.1227948)
37. Bonin MC, Almany GR, Jones GP. 2011 Contrasting effects of habitat loss and fragmentation on coral-associated reef fishes. *Ecology* **92**, 1503–1512. (doi:10.1890/10-0627.1)
38. Schindler DE, Scheuerell MD. 2002 Habitat coupling in lake ecosystems. *Oikos* **98**, 177–189. (doi:10.1034/j.1600-0706.2002.980201.x)
39. Choat JH, Clements KD, Robbins WD. 2002 The trophic status of herbivorous fishes on coral reefs. *Mar. Biol.* **140**, 613–623. (doi:10.1007/s00227-001-0715-3)
40. Rurua V, Béarez P, Hermann A, Conte E. 2020 Length and weight reconstruction of *Chlorurus microrhinos* (Scaridae) from isolated cranial bones and vertebrae. *Cybium* **44**, 61–68. (doi:10.26028/cybium/2020-441-008)
41. Welsh JQ, Bellwood DR. 2012 Spatial ecology of the steephead parrotfish (*Chlorurus microrhinos*): an evaluation using acoustic telemetry. *Coral Reefs* **31**, 55–65. (doi:10.1007/s00338-011-0813-8)
42. Cruz-Escalona VH, Peterson MS, Campos-Davila L, Zetina-Rejon M. 2005 Feeding habits and trophic morphology of inshore lizardfish (*Synodus foetens*) on the central continental shelf off Veracruz, Gulf of Mexico. *J. Appl. Ichthyol.* **21**, 525–530. (doi:10.1111/j.1439-0426.2005.00651.x)
43. Coker DJ, Hoey AS, Wilson SK, Depczynski M, Graham NAJ, Hobbs JPA, Holmes TH, Pratchett MS. 2015 Habitat selectivity and reliance on live corals for Indo-Pacific hawkfishes (family: Cirrhitidae). *PLoS One* **10**, e0138136. (doi:10.1371/journal.pone.0138136)
44. Brandl SJ, Goatley CHR, Bellwood DR, Tornabene L. 2018 The hidden half: ecology and evolution of cryptobenthic fishes on coral reefs. *Biol. Rev.* **93**, 1846–1873. (doi:10.1111/brv.12423)
45. Siqueira AC, Morais RA, Bellwood DR, Cowman PF. 2020 Trophic innovations fuel reef fish diversification. *Nat. Commun.* **11**, 2669. (doi:10.1038/s41467-020-16498-w)
46. Talmy D, Carr E, Rajakaruna H, Vage S, Willem-Omta A. 2023 Killing the predator: impacts of top predator mortality on global-ocean ecosystem structure. *Biogeosci. Discuss.* **21**, 1–29. (doi:10.5194/bg-2023-120)
47. Schmitt RJ, Holbrook SJ, Brooks AJ, Lape JCP. 2009 Intraguild predation in a structured habitat: distinguishing multiple-predator effects from competitor effects. *Ecology* **90**, 2434–2443. (doi:10.1890/08-1225.1)
48. Manica A. 2002 Filial cannibalism in teleost fish. *Biol. Rev.* **77**, 261–277. (doi:10.1017\S1464793101005905)
49. Hatton IA, Heneghan RF, Bar-On YM, Galbraith ED. 2021 The global ocean size spectrum from bacteria to whales. *Sci. Adv.* **7**, 1–12. (doi:10.1126/sciadv.abh3732)
50. Brandl S *et al*. 2019 Demographic dynamics of the smallest marine vertebrates fuel coral reef ecosystem functioning. *Science (1979)* **364**, 1189–1192. (doi:10.2307/26681652)
51. Barneche DR, Kulbicki M, Floeter SR, Friedlander AM, Maina J, Allen AP. 2014 Scaling metabolism from individuals to reef-fish communities at broad spatial scales. *Ecol. Lett.* **17**, 1067–1076. (doi:10.1111/ele.12309)
52. Morais RA, Bellwood DR. 2019 Pelagic subsidies underpin fish productivity on a degraded coral reef. *Curr. Biol.* **29**, 1521–1527. (doi:10.1016/j.cub.2019.03.044)
53. Heather FJ, Blanchard JL, Edgar GJ, Trebilco R, Stuart-Smith RD. 2021 Globally consistent reef size spectra integrating fishes and invertebrates. *Ecol. Lett.* **24**, 572–579. (doi:10.1111/ele.13661)
54. Froese R, Pauly D. 2024 FishBase. See https://www.fishbase.org/.
55. Ackerman JD. 1999 Effect of velocity on the filter feeding of dreissenid mussels (*Dreissena polymorpha* and *Dreissena bugensis*): implications for trophic dynamics. *Can. J. Fish. Aquat. Sci.* **56**, 1551–1561. (doi:10.1139/f99-079)
56. Kulbicki M, Wantiez L, Thollot P, Tham GM. 2022 Functional and taxonomic overlap in shore fish assemblages in a tropical seascape. Diversity (Basel) **14**, 310. (doi:10.3390/d14050310)
57. Carassou L, Kulbicki M, Nicola TJR, Polunin NVC. 2008 Assessment of fish trophic status and relationships by stable isotope data in the coral reef lagoon of New Caledonia, southwest Pacific. *Aquat. Living Resour.* **21**, 1–12. (doi:10.1051/alr:2008017)
58. Bürkner PC. 2021 Bayesian item response modeling in R with brms and Stan. *J. Stat. Softw.* **100**, 1–54. (doi:10.18637/jss.v100.i05)
59. Post DM. 2002 Using stable isotopes to estimate trophic position: models, methods, and assumptions. *Ecology* **83**, 703. (doi:10.2307/3071875)
60. R Core Team. 2024 R: a language and environment for statistical computing. Vienna, Austria: R Foundation for Statistical Computing.
61. Gelman A, Goodrich B, Gabry J, Vehtari A. 2019 R-squared for Bayesian regression models. *Am. Stat.* **73**, 307–309. (doi:10.1080/00031305.2018.1549100)
62. Gabry J, Goodrich B, Lysy M, Johnson A. 2024 rstantools: Tools for developing R packages interfacing with 'Stan'. See https://CRAN.R-project.org/package=rstantools.
63. Delecambre Z, Parravicini V. 2025 Data from: Weak trophic position–body mass relationships undermine simple size spectrum models for coral reefs. Dryad Digital Repository. (doi:10.5061/dryad.tmpg4f58c)
64. Delecambre Z, Ghilardi M, Diego RB, Adjeroud M, Brandl SJ, Casey JM *et al*. 2026 Supplementary material from: Weak trophic position-body mass relationships undermine simple size spectrum models for coral reefs. Figshare. (doi:10.6084/m9.figshare.c.8257816)